doi:10.1007/s11589-011-0805-3

Thermal structure about southwest sub-basin of South China Sea*

Lin Meng♦ and Jian Zhang

Laboratory of Computational Geodynamics, The Graduate University of the Chinese Academy of Sciences, Beijing 100049, *China*

Abstract There are some factors, such as the topographic relief, sedimentary thickness and thermal conductivity, magmatic activity and thermal cooling, influencing the seafloor heat flow and the evolution of lithosphere structure in southwest sub-basin (SWSB), South China Sea. On the base of the geological structure characteristic of SWSB this paper will discuss some other factors including thermal anomaly area, dike produced by magma intrusion and lithosphere relief, by modeling and calculating. Calculating results indicate partial areas where temperature is higher than vicinity in the lithosphere, which we call thermal anomaly here containing thermal anomaly area and dike in this paper, could decrease heat flow below, increase above, and gradually increase to two sides; heat flow in upwelling parts of lithosphere is usually higher than sinking parts, and in the middle is of a gradual transition.

Key words: **southwest sub-basin (SWSB); thermal anomaly field; heat flow; dike; lithosphere relief**
CLC number: P314 **Document code**: A

1 Introduction

There are closely relationship between thermal structure of lithosphere and magmatic activity, and not only transport path of magma but also dynamical resource of transport is the key point on researching transport dynamics of magma (Qiu, 1985; Xu et al., 2006; Liu et al., 2004; Niu et al., 1996). Magmatic melting and underground structure of viscosity are both related to the structure of temperature, so we can say that magmatic activity is restricted by thermal structure of lithosphere. On the other hand, magmatic activity also influences temperature structure and heat flow distributions of lithosphere. Zhang et al. (2005) drew a conclusion by way of thermal modeling, that the rate of magma supply had an equal magnitude with the seafloor spreading rate of SWSB. Meanwhile, he thought that southwest sub-basin (SWSB) might only last for 10 to 15 Ma. Zhang et al. 's study just showed the relationship between thermal structure of lithosphere and magmatic activity. There are many seamounts in South China Sea Basins (SCSB). Lots of works about seamounts have been done, and it is still one of the hottest research topics now. Seamounts are often accompanied by magmatic activity. Wang et al. (2009) studied the magmatic activity of Zhenbei-Huangyan seamount in SCSB using geochemical method. Using the same method, Yang et al. (2011) researched magma evolution of seamount by analyzing seamount volcanic rocks in central sub-basin, South China Sea. Their geochemical results can supply information for seamount research related to lithosphere thermal structure using the method of geophysics. There are seamounts that may be produced by magmatic activity in SWSB, as we can see in Figure 1. Besides, some other researchers also made great much work on thermal structure of lithosphere elsewhere (Zang et al., 2002a, b; Chi and Yan, 1998; Liu et al., 2003; Shi et al., 2003). This paper will discuss the influence factors of lithosphere thermal structure, including thermal anomaly and lithosphere relief, with the modeling method of finite element analysis at the base of FEPG software. We will put heat flow as the key researching object because it is a most important physical parameter of thermal structure, and discuss its influence factors

* **Received** 30 August 2011; **accepted in revised form** 20 September 2011; **published** 10 October 2011.
♦ **Corresponding author. e-mail**: menglin09@mails.gucas.ac.cn

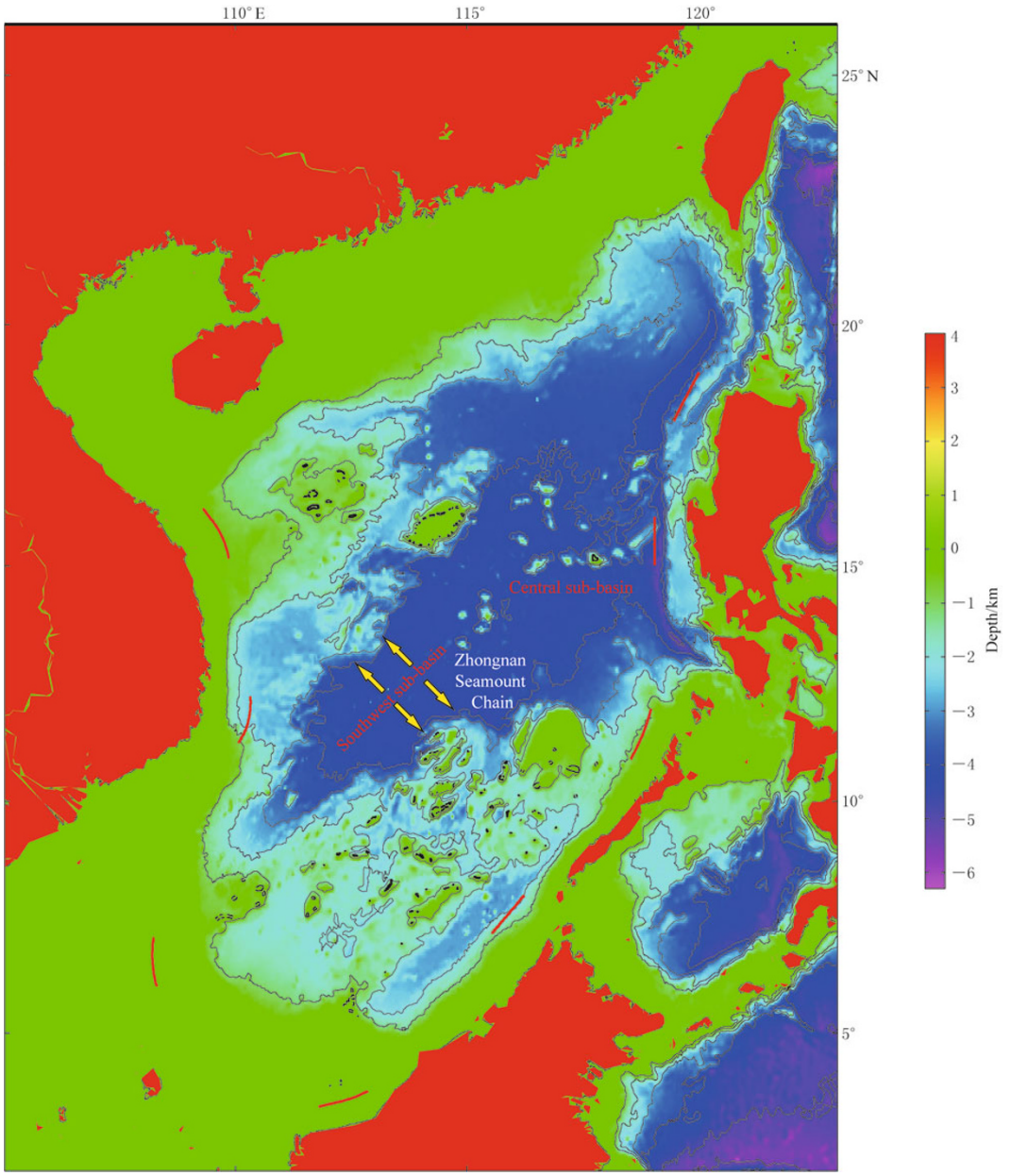

Figure 1 Schematic diagram of SWSB location. The yellow arrow indicates spreading direction NW-SE. Red color represent areas within the continental coastline.

with different models. This research will provide preparations for building thermal structure model of lithosphere under SWSB. The physical parameters of the thermal structure contain thermal conductivity, rate of heat generation, temperature, heat flow and so on, among which temperature and heat flow are the most important ones to describe the characteristics of thermal structure. Temperature is the fundamental parameter influencing lithosphere deformation, viscosity structure, magma melting and magma transport. However, the heat flow generated by heat supply at the bottom of lithosphere and the heat flow dissipated at seafloor has both close relationship and mutual influences with temperature.

2 Geological background

South China Sea is located at the intersection of Eurasian plate, Indian-Australian plate and Philippine plate, containing central sub-basin in the east, northwest sub-basin and SWSB as shown in Figure 1. SWSB

is to the southwest of the central sub-basin. They are separated by Zhongnan Seamount Chain, which is along approximately north-south direction. The depth of water in SWSB ranges from 3000 to 4400 m, the lowest part in South China Sea. SWSB has a NW-SE spreading direction and near-flank topography. People almost hold the same viewpoint on the spreading time of central sub-basin, between 32 to 17 Ma ago, but they still do not make an agreement on the spreading time of SWSB. Hayes et al. (1987), Hayes (1990) and Briais et al. (1993) thought spreading happened between 24 to 15.5 Ma ago, which is correspond to middle-to-late period of central sub-basin spreading stage by multi-wave analysis and geomagnetic data comparison. Taylor and Hayes (1980, 1983) drew a conclusion that SWSB has the same spreading period with central sub-basin using geomagnetic anomaly and gravity data. Chen (1987), Lu (1987) and Yao (1996) holds the spreading time of 126–119 Ma, 70–63 Ma and 42–35 Ma, respectively. However, we don't care the spreading time in this paper for it is not strongly related to our research.

Yao (1999) thought the seamounts in SWSB may be produced by volcanic eruption. That means magma chamber may exist in the lithosphere. Zhang et al. (2005)'s research on tectonic evolution by thermal simulation also provided evidence to the existing of magma chamber in SWSB. Zhao et al. (2011) brought forward a point that there's magma chamber under residual ocean ridges by researching seamount characteristics of South China Sea Basin. There is little seafloor heat flow data (He, 1998). Using geothermal method Zhang et al. (2001) calculated that, the temperature ranged from 100°C to 600°C at sedimentary basement, 600°C to 1 000°C at Moho, 1 150°C to 1 300°C at the bottom of lithosphere in South China Sea, and the temperature of interface between upper and lower mantle of central sub-basin, which is near the southwest basin, ranges from 400°C to 800°C. The surface heat flow of southwest basin is high, about 100 to 150 mW/m^2, and has a descending trend from northwest to southeast. Deposit's thickness ranges from 0.28 to 0.72 km, crust from 10 to 20 km and lithosphere from 28 to 40 km. The thickness of crust and lithosphere both have an increasing trend from center to two sides (Zhang et al., 2005; Chen and Lin, 1997).

We suppose the thermal structure of SWSB is in a stable state, so we will consider the situation of thermal static conduction in calculating process. Model (1) is a 2D model with four equal thickness layers. The result shows that the lithosphere heat flow is distributed uniformly in the horizontal direction, and the bottom heat flow is higher than 100 mW/m^2. However, in fact the thickness of each layer is laterally heterogenous. So according to the geological structure data, we build model (2), whose layer thickness is varying. Model (2) is more realistic than model (1), and the influence of lithosphere relief is considered in model (2). The result of model (2) simulation indicates that the lithosphere heat flow is also not uniform, gradually decreasing from middle to both sides. However, the minimum of bottom heat flow is still higher than 50 mW/m^2, at the ends of model. According to some researching result the current bottom heat flow of SWSB is about 30 mW/m^2 (Zhang et al., 2005), which is much lower than the result of model (2), so we add a thermal anomaly area to represent the existence of magma chamber, and add a thermal anomaly line to represent dike. This is model (3). In this model we considered the influence of thermal anomaly field. In all the three models, the temperature of the surface maintains 8°C, and the temperature of bottom maintains 1 200°C.

3 Method

Our simulation method is mainly based on the static-state heat conduction equation (1) and heat flow calculation formula (2), which are expressed below:

$$-k\nabla^2 T = A, \tag{1}$$

$$q = -k\nabla T, \tag{2}$$

In the formulas, k represents thermal conductivity, A represents heat generation rate, T represents temperature, and q represents heat flow. Three models all have an x-direction length and a z-direction height, and they all have four layers called layer 1, layer 2, layer 3 and layer 4 from top to bottom.

Model (1) is 200 km long in NW-SE direction and 30 km high in vertical direction, all the four layers are flank and each has a equal thickness of 1, 5, 4 and 20 km, respectively. The model is divided into 10 807 quadrilateral finite element computational grids. According to Gemmer and Scren (2002) and Zhang et al. (2005), we set the boundary conditions as below: surface temperature is 8°C; bottom temperature is 1 200°C; both ends of sides are free boundary as shown in Figure 2a.

Model (2) is 200 km long in NW-SE direction. Total thickness ranges from 17.7 km to 40 km with each layer changing laterally. According to the geological background of the SWSB above, the layer thickness ranges are designed as Table 1. Each layer is thickening

from middle to both sides, and the boundaries between each of two adjacent layers are all circular shape except the boundary between layer 1 and 2 which is a line. Model (2) is divided into 11 680 triangular finite element computational grids. It has the same boundary conditions as model (1). See Figure 2b.

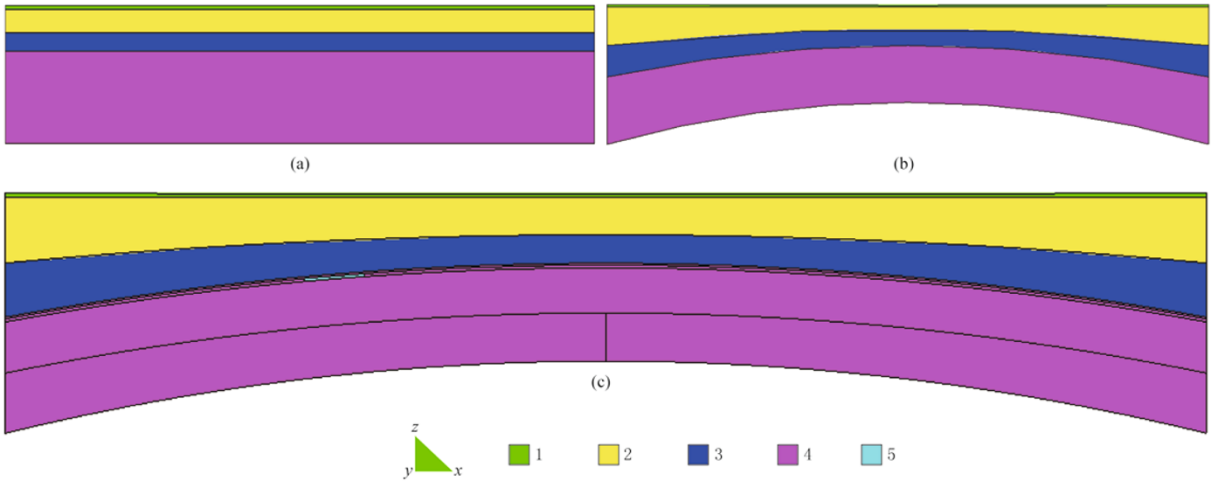

Figure 2 Models. (a) Model (1), thickness of each layer is uniform; (b) model (2), thickness of each layer is changing with space; (c) model (3), add a high-temperature area and a high-temperature line.

Table 1 Model parameters

Parameter	Layer 1	Layer 2	Layer 3	Layer 4
Thermal conductivity/(W·m^{-1}·°C^{-1})	0.85	3.0	2.3	3.3
Density/(kg·m^{-3})	2 380	2 770	2 830	3 190
Heat capacity/(W·kg^{-1}·°C^{-1})	900	900	900	1 000
Heat generation rate/(μW·m^{-3})	1.28e−6	1.3e−6	0.4e−6	0.024e−6
Thickness rage/km	0.4−0.7	6−11	5−9	6.3−19.3

Model (3) is the most realistic model of three, because it considers thermal anomaly influence by adding high temperature parts, which represent the possible geological bodies such as magma chamber and dike. Compared with model (2), model (3) has a simulated high-temperature quadrilateral area (color 5) on the top left side and has an 8 km long, vertical high-temperature line under the middle. The two thermal anomaly fields are all set to 1 200°C. Actually, the temperature of thermal anomaly area maybe higher than the temperature of line, and the temperature of magma chamber is changing with various types of rock produced which can also result in the inaccuracy of our set temperature, but they don't affect the result here. The area is 10 km long and 1.2 km high. It ranges from −50 to −40 km in horizontal direction and from 14.7 to 13.5 km in vertical direction. This region corresponds to 950°C to 1 050°C in temperature profile of model (2). The model is divided into 36 414 triangular finite element computational grids. Boundary conditions are almost the same as that in model (1), except that the high-temperature area and line are set to 1 200°C as shown in Figure 2c.

All the steady-state results containing temperature structure and heat flow distribution, based on the three models above, are all calculated by formula (1). Model parameters include thermal conductivity, density, heat capacity, heat generation rate and layer thickness, as shown in Table 1. All the parameters are from Zhang's document (Zhang et al., 2005).

4 Results and discussion

4.1 Influencing factor of thermal structure

In this part, all the models including thermal anomaly area model (Figure 3), dike model (Figure 4a) and lithosphere relief model (Figure 4b), are all 2D model with four equal thickness layers. Thermal anomaly model adds two high-temperature areas at the base of

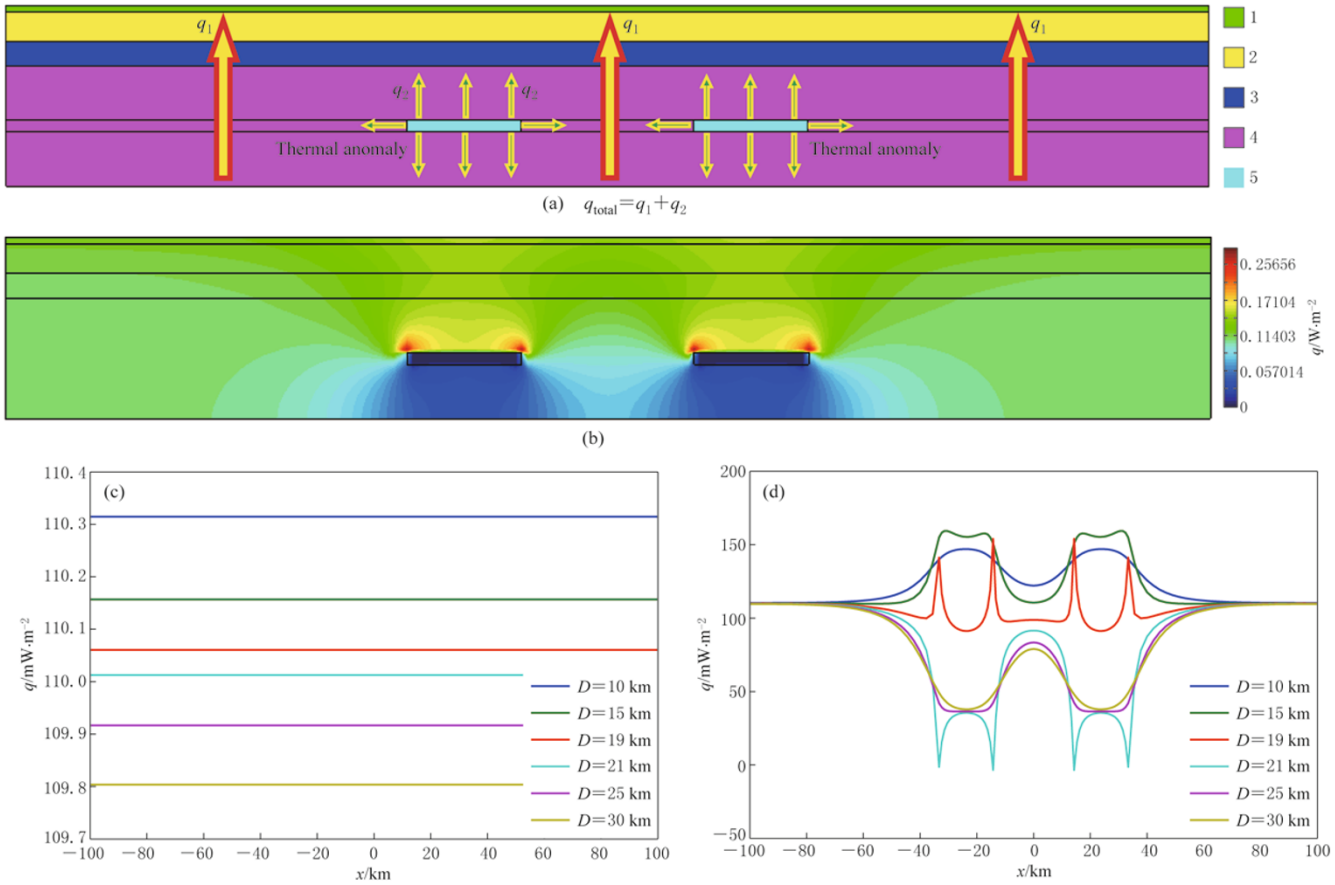

Figure 3 The consequence of thermal anomaly field. (a) Model of thermal anomaly field; (b) profile of heat flow; (c) no thermal anomaly field; variation of heat flow versus x-axis at different depths; (d) existing thermal anomaly field; variation of heat flow versus x-axis at different depths.

model (1). Dike model adds a high-temperature line at the base of model (1). The position of those thermal anomaly fields need not be cared because we only analyze the influence of thermal anomaly qualitatively. In lithosphere model the bottom is fluctuated with three sinking parts and two upwelling parts compared to model (1). The sinking and upwelling amplitude is small.

4.1.1 Influence of thermal anomaly area

Figure 3a shows the model with thermal anomaly fields. There are two high-temperature areas with a quadrilateral shape in the model. They are 19 km long and 2 km thick, and the anomaly temperature is set to 1 100°C which is higher than the vicinity. Figure 3b shows the corresponding profile of heat flow. We can see that, the temperature is uniform and the heat flow equals to zero inside high-temperature areas. The heat flow is lower below the anomaly area than the vicinity, higher above, a little lower at two sides and increasing to both sides laterally. Figures 3c and 3d each shows the heat flow in the case of having no thermal anomaly area and having thermal anomaly area. Comparing Figures 3c and 3d we can see that, above the anomaly area the heat flow have an inhomogeneous increase, like curves D=10 km, D=15 km and D=19 km; while below the anomaly area the heat flow have an inhomogeneous decrease, as shown by curves D=21 km, D=25 km and D=30 km. On the top of thermal anomaly areas heat flow increases in the largest amplitude, corresponding to the uplift position in Figure 3d; while at the bottom decreases in the largest amplitude, corresponding to the depressed position in Figure 3d. The reason of resulting in the heat flow increasing above the thermal anomaly area, maybe that temperature gradient resulted from anomaly area is superimposed with the upward temperature gradient in the original structure of temperature, performing that q_2 and q_1 have the same direction in Figure 3a; in contrast, The reason of resulting in the heat flow decreasing below the thermal anomaly area, maybe that temperature gradient resulted from anomaly area counteract the upward temperature gradient in

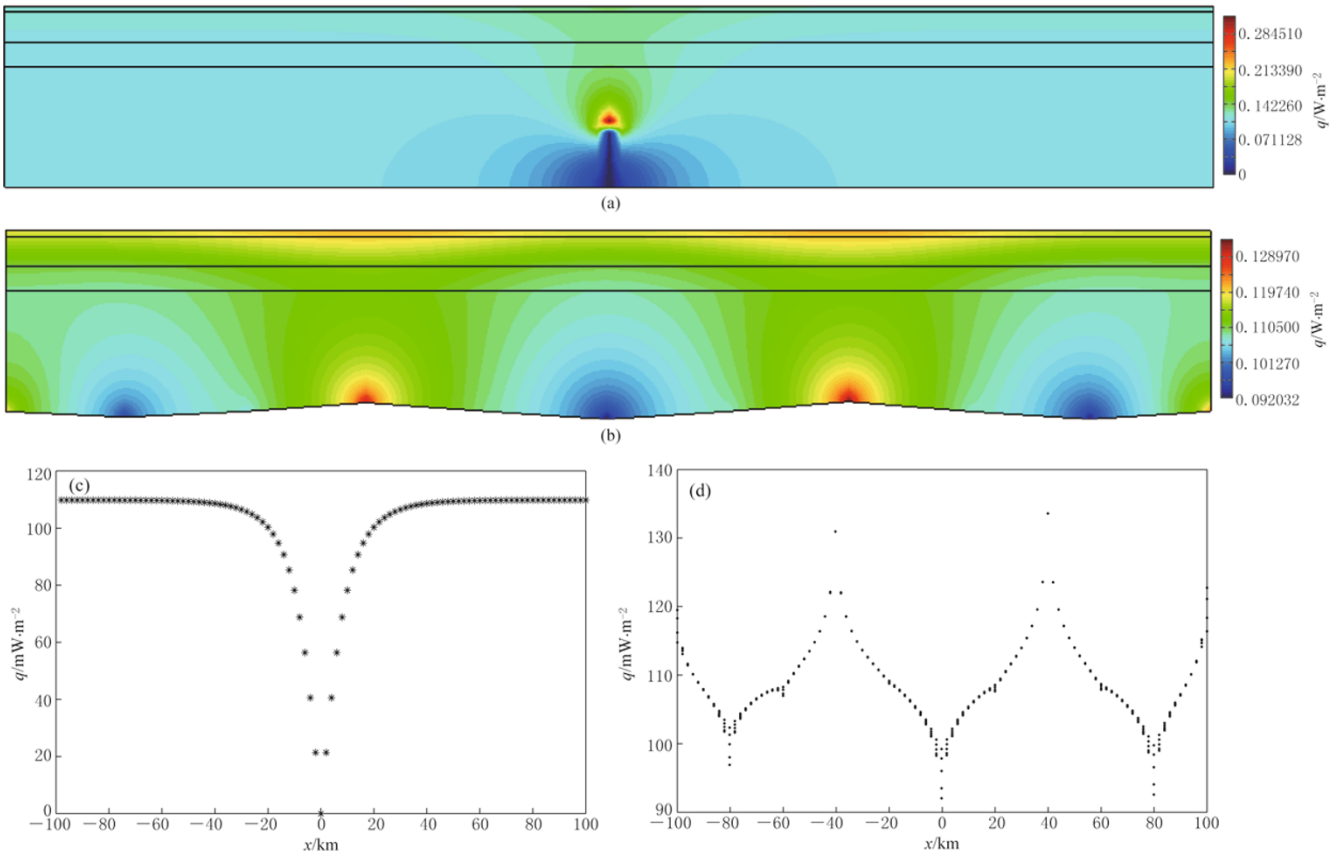

Figure 4 The consequence of dike and structure relief. (a) Heat flow profile resulting from dike; (b) heat flow profile resulting from structure relief; (c) variation of heat flow versus x-axis at the bottom of lithosphere; (d) variation of heat flow versus x-axis at the bottom of lithosphere corresponding to (a).

the original structure of temperature, performing that q_2 and q_1 have the opposite direction in Figure 3a.

4.1.2 Influence of dike and lithosphere relief

Dike is a phenomenon of magmatic upwelling. Upwelling material, that produces dike, has a higher temperature than normal upper mantle, so we can regard dike as a case of thermal anomaly. According to section 4.1.1 we can infer that, heat flow above dike is higher than vicinity, lower at two sides, and increasing to both sides laterally. Figure 4a shows the simulated result. Inside dike the heat flow is zero, and increases from dike to both two sides laterally. That is in accordance with our inference.

The relief of lithosphere surface, bottom and interfaces between each two layers all influence the thermal structure of lithosphere. Here we only consider the influence of lithosphere bottom relief. Lithosphere relief could make isotherm curving. At the same level of depth upwelling parts have higher temperature than sinking parts, so the two upwelling parts can also be regarded as the case of thermal anomaly in some sense. We can infer that below the upwelling parts the heat flow is lower, obviously the three sinking parts should have lower value of heat flow, and that is just reflected in the blue areas of Figure 4b. We can also infer above the upwelling parts the heat flow is higher, and it is well in accordance with the red area in Figure 4b. The result of our inference and simulation is consistent. According to the analysis above we can draw conclusions about the surface and bottom heat flow as below. In the surface heat flow profile of dike the value on top of dike is higher than two sides, and in the bottom heat flow profile the value increasing from dike to both two sides. In the surface heat flow profile of lithosphere relief the value on the top of upwelling parts is higher than the sinking parts, and in the bottom heat flow profile the value of upwelling parts is higher, sinking parts is lower, and in the middle is of gradual transition. In this paper we only lay out the bottom profile of dike and lithosphere bottom relief as shown in Figures 4c and 4d.

4.2 Analysis about models

Thickness of each layer is uniform in model (1) but changing in model (2). Therefore, in the sense of geological structure of lithosphere, model (2) is better than model (1) to represent actual SWSB. In terms of lithosphere thickness, it is about 12 km thinner in the center than that at the ends in model (2), so the temperature gradient in the center is larger than that at the ends. According to formula (2), the heat flow in the center is higher than that at the ends. In the viewpoint of lithosphere relief, the center of the model (2) corresponds to upwelling parts and the ends correspond to sinking parts. According to the analysis above upwelling parts have a higher heat flow than sinking parts, so the heat flow in the center should be higher than that at the ends. In terms of thermal anomaly, because the temperature in the center of model (2) is higher than two flanks at the same level of depth, the central position can be seen as an anomaly field comparing to two sides, with a performance of lower heat flow at the ends than that in the center. Not only in the case of lithosphere thickness but also in the case of lithosphere relief and thermal anomaly field, the result of heat flow at two ends of model (2) are both lower than that in the center as shown in Figure 5b. Figure 5c shows heat flow changes at seafloor with a heat flow difference of 30 mW/m^2 in the center and at the ends, and Figure 5d shows heat flow, with a minimum value of about 50 mW/m^2, changes at the bottom of lithosphere with a heat flow difference of 80 mW/m^2. But what we are interested here is that the bottom heat flow should decrease to 30 mW/m^2 or lower. The heat flow in model (1) is horizontally uniform as shown in Figure 5a.

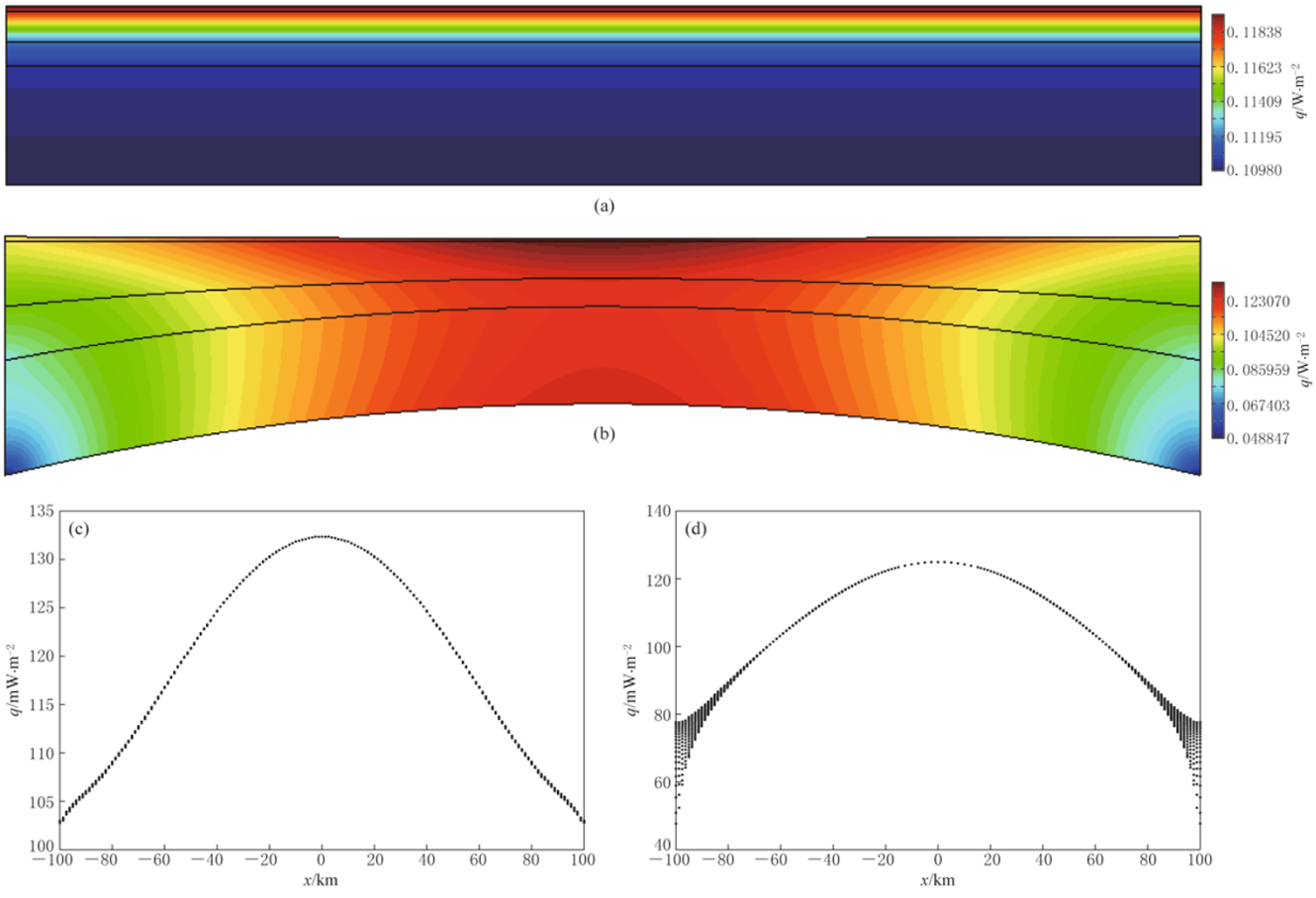

Figure 5 Comparative map of heat flow. (a) Heat flow profile of model (1); (b) heat flow profile of model (2); (c) variation of surface heat flow versus x-axis in model (2); (d) variation of bottom heat flow versus x-axis in model (2).

According to actual data, seafloor heat flow of SWSB in South China Sea is between 100 to 150 mW/m^2 with a decreasing trend from northwest to southeast, and the heat flow at the bottom of lithosphere is about 30 mW/m^2 or lower (Zhang et al., 2005). Though the heat flow of seafloor is in accordance with the actual data, the trend exists deviation and the heat flow at the bottom of lithosphere is still higher than 50 mW/m^2 which is much higher than 30 mW/m^2. So we build model (3) to approach the more realistic situation. Compared to model (2) the main characteristic of model (3) is that, there is a simulated high-temperature quadrilateral area on the top left side to represent magma chamber and a vertical high-temperature line under the middle to represent dike. In this paper we consider magma chamber and dike as thermal anomaly field. According to researches before, we know that there are chambers under SWSB very likely, which would result in the seafloor heat flow above chambers increase and bottom heat flow below chambers decrease. As seafloor heat flow decreases from NW to SE according to actual data, we set the high-temperature area at the left side deliberately. The calculated result of heat flow profile shows, somewhere above the thermal anomaly field, the heat flow is higher than 150 mW/m^2, which is corresponding to the position of "vacant" in Figure 6a. However, there's a decreasing trend of heat flow from the top of thermal anomaly (x=−45 km) to southeast except partial increase resulting from dike as shown in Figure 6b. That is one of our interested results. Additionally, model (3) results in a further heat flow decrease partially compared to the result of model (2), at the bottom of the lithosphere as shown in Figure 6c, with the value even decreasing to 30 mW/ m^2 or lower. That's another interesting result for us. The linear thermal anomaly field causes the bottom heat flow decrease, too. There're magma chambers and dikes existing in SWSB. The chambers and dikes can be seen as thermal anomaly fields, which can make the bottom heat flow decrease and make the seafloor heat flow increase, partially. If chambers and dikes are all in proper positions, it will result in the decreasing trend from northwest to southeast as actual data.

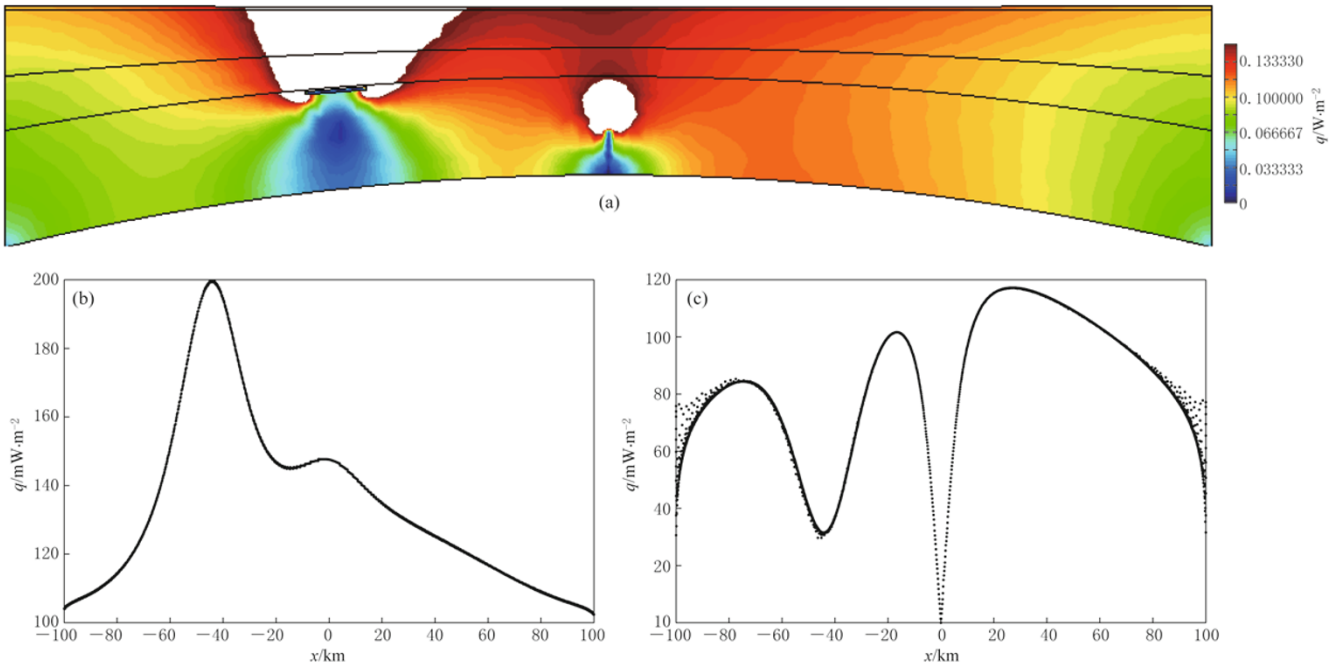

Figure 6 Heat flow curves of model (3). (a) Profile of heat flow; (b) variation of heat flow versus x-axis on seafloor; (c) variation of heat flow versus x-axis seafloor at the bottom of lithosphere.

According to the influences analyzed above, model (3) still has deficiencies as bellow. (1) The thickness of all layers is not accordant with the reality. The actual layers may not be as smooth as the model. With the influence of lithosphere relief the results of model (3) is not accuracy. (2) The positions of thermal anomaly fields are not in accordance with the reality. This paper is just to illustrate that thermal anomaly fields

such as magma chambers and dikes could influence the heat flow, so we should build corresponding model based on the actual geological data. Except for the two influence factors researched above, some other factors such as thermal conductivity and thermal cooling can also affect the result of simulation. Firstly, thermal conductivities in this paper are not accordant with the reality. In this paper we suppose the conductivity of each layer is constant, but the value is usually changing with temperature, pressure or different mineral composition (Liu et al., 2003; Wang et al., 1996; Zang et al., 2002b; Ou et al., 2006). According to formula (2), the conductivity can affect the heat flow. Secondly, the result of calculation is in the case of static state heat conduction, and we don't consider the process of thermal cooling, while SWSB of South China Sea has gone through seafloor spreading stage and thermal cooling stage according to previous studies. The heat flow of lithosphere will decrease at the stage of thermal cooling.

5 Conclusions

By numerical simulation and comparing the result with actual data of SWSB in South China Sea we can draw conclusions as follows:

1) Thermal anomaly area could increase the heat flow above, decrease below, and increase to both sides. Accordingly, it can increase the seafloor heat flow and decrease the bottom heat flow of lithosphere. The reason of resulting in the heat flow increasing above the thermal anomaly area maybe that, temperature gradient resulted from anomaly area is superimposed with the upward temperature gradient in the original structure of temperature; in contrast, The reason of resulting in the heat flow decreasing below the thermal anomaly area maybe that temperature gradient resulted from anomaly area counteract the upward temperature gradient in the original structure of temperature.

2) Heat flow above dike is higher than vicinity, lower at two sides and increasing to both sides laterally. Dike could make both seafloor heat flow and bottom heat flow of lithosphere increase from the dike to two sides laterally. Dike can be seen as a special case of geological thermal fields.

3) Lithosphere relief could influence heat flow distribution. Taking the bottom of lithosphere as an example, at the same level of depth upwelling parts have higher temperature than sinking parts, so upwelling parts can be regarded as the case of thermal anomaly in some sense. The heat flow below the upwelling parts is lower and above is higher. The value of seafloor heat flow on the top of upwelling parts is higher than the sinking parts. At the bottom heat flow profile the value of upwelling parts is higher, sinking parts is lower, and in the middle is of gradual transition.

4) Comparison of three models well reflected the influence of thermal anomaly field and lithosphere relief to heat flow of lithosphere. By comparing the results of simulation with actual data we can deserve that, besides variation of layer thickness, layer conductivity and thermal cooling process, some other influence factors such as magma chamber, dike, and lithosphere relief should also be considered to build the lithosphere thermal structure of SWSB in South China Sea.

Acknowledgements I would like to express my sincere gratitude to the two anonymous reviewers for their valuable comments on this paper. Thanks are also given to my dear tutor for giving me many advices in completing this paper.

References

Briais A, Patrizt P and Tapponnier P (1993). Updated interpretation of magnetic anomalies and seafloor spreading stages in the South China Sea: Implications for the tertiary tectonics of Southeast Asia. *J Geophys Tes* **98**: 6 299–6 328.

Chen S Y (1987). The magnetic anomaly map of South China Sea. Guangdong Atlas Press, Guangzhou (in Chinese).

Chen X and Lin J F (1997). An analysis of the lithospheric thickness and crustal age in the center sub-basin of South China Sea. *Acta Oceanologica Sinica* **19**(2): 71–84 (in Chinese with English abstract).

Chi Q H and Yan M C (1998). Radioactive elements of rocks in North China platform and the thermal structure and temperature distribution of the modern continental lithosphere. *Chinese J Geophys* **41**(1): 38–47 (in Chinese with English abstract).

Gemmer L and Scren B (2002). Post-mid-Cretaceous eastern North Sea evolution inferred from 3D thermo-mechanical modeling. *Tectonophysics* **350**: 315–342.

Hayes D E, Spangler S, Yao B and Zeng W (1987). Age and evolution of the South China Sea southwest sub-basin. *EOS Trans*, *AGU*, **68**: 1 496.

Hayes D E (1990). The tectonic evolution of the Great South China Sea. *AAPG Bull* **74**: 978.

He L J, Xiong L P and Wang J Y (1998). The geothermal characteristics in South China Sea. *China Offshore Oil and Gas* (*Geology*) **12**(2): 87–90.

Liu H T, Zhang Q, Liu J M, Ye J, Zeng Q D and Yu C M (2004). Adakite versus porphyry copper and epithermal gold deposits: A possible metallogenetic specialization of

magmatism required in-deep assessment. *Acta Petrologica Sinica* **20**(2): 205–218.

Liu S W, Wang L S, Li C, Li H, Han Y B, Jia C Z and Wei G Q (2003). Lithspheric thermal-rheological structure of lithosphere and at the northern edge of Tarim, China. *Science in China* (*Series D*) **33**(9): 852–863.

Lu Z W (1987). The character of magnetic belt and tectonic evolution in the center sub-basin of South China Sea. *Acta Oceanologica Sinica* **9**(1): 69–78 (in Chinese).

Niu S Y, Li H Y, Sun A Q, Luo M W, Ye D H and Wang J S (1996). Multistage evolution and mineralization of mantle plume as exemplified by Northern Hebet area. *Mineral Deposits* **15**(4): 298–306.

Ou X G, Jin X M, Xia B, Xu H J and Jin S Y (2006). Prediction of thermal conductivity of underground rocks from P-wave velocity of ultrahigh-pressure metamorphic rocks. *Earth Science—Journal of China University of Geosciences* **31**(4): 564–568.

Qiu J X (1985). *Dynamics of Magmatic Rocks*. Geological Publishing House, Beijing, 251–279 (in Chinese).

Shi X B, Qiu X L, Xia K Y and Zhou D (2003). Heat flow characteristics and its tectonic significance of South China Sea. *Journal of Tropical Oceanography* **22**(2): 63–73.

Taylor B and Hayes D E (1980). The tectonic evolution of the South China Sea Basin. In: Hayes DE ed. *The Tectonic and Geological Evolution of Southeast Asian Seas and Islands*. AGU, Geophysical Monogrqaph **23**: 89–104.

Taylor B and Hayes D E (1983). Origin and history of the South China Sea Basin. In: Hayes D E ed. *The Tectonic and Geological Evolution of Southeast Asian Seas and Islands*. AGU, Geophysical Monogrqaph, **27**: 23–56.

Wang L S, Li C and Yang C (1996). The lithospheric thermal structure beneath Tarim Basin,Western China. *Chinese J Geophys* **39**(6): 794–803 (in Chinese with English abstract).

Wang Y J, Han X Q, Luo Z H, Qiu Z Y, Ding W W, Li J B, Gao S T and Chen R H (2009). Late Miocene magmatism and evolution of Zhenbei-Huangyan Seamount in the South China Sea: Evidence from petrochemistry and chronology. *Acta Oceanologica Sinica* **31**(4): 93–101 (in Chinese with English abstract).

Xu X W, Wang J, Zhang B L, Qing K Z and Cai X P (2006). Transport dynamics of magma and its advances. *Advances in Earth Science* **21**(4): 361–371.

Yang S Y, Fang N Q, Yang S X, Yao B C and Liang D H (2011). A further discussion on formation background and tectonic constraints of igneous rocks in Central Sub-Basin of the South China Sea. *Earth Science — Journal of China University of Geosciences* **36**(3): 455–470.

Yao B C (1996). Tectonic characteristics and evolution of the Nansha Trough. *Geological Research of South China Sea* **9**(1): 69–78 (in Chinese with English abstract).

Yao B C (1999). On the lithospheric rifting model in the southwest sub-basin of South China Sea. *Marine Geology and Quaternary Geology* **19**(2): 37–47 (in Chinese with English abstract).

Zang S X, Li C, Ning J Y, and Wei R Q (2002a). A preliminary model about 3D rheological structure of lithosphere in North China. *Science in China* (*Series D*) **32**(7): 588–597.

Zang S X, Liu Y G and Ning J Y (2002b). Thermal structure of the lithosphere in North China. *Chinese J Geophys* **45**(1): 56–66 (in Chinese with English abstract).

Zhang J, Song H B and Li J B (2005). Thermal modeling of the tectonic evolution of the SWSB in the South China Sea. *Chinese J Geophys* **48**(6): 1 357–1 365 (in Chinese with English abstract).

Zhang J, Xiong L P and Wang J Y (2001). Characteristics and methanism of geodynamic evolution of the South China Sea. *Chinese J Geophys* **44**(5): 602–610 (in Chinese with English abstract).

Zhao M H, Qiu X L, Xu, H L, Xia S H, Wu Z L, Li J B (2011). Deep seismic surveys in the Southern South China Sea and contrast on its conjugate margins. *Earth Science — Journal of China University of Geosciences* **36**(5): 823–830.